Superconductivity and structural variation of the electron-correlated layer systems $Sr(Pd_{1-x}T_x)_2Ge_2$ (T = Co, Ni, Rh; $0 \leqslant x \leqslant 1$)

J. W. Wang, I. A. Chen, T. L. Hung, Y. B. You, and H. C. Ku*
Department of Physics, National Tsing Hua University, Hsinchu 30013, Taiwan, Republic of China

Y. Y. Hsu
Department of Physics, National Taiwan Normal University, Taipei 10677, Taiwan, Republic of China

J. C. Ho
Department of Physics, Wichita State University, Wichita, Kansas 67260-0032, USA

Y. Y. Chen
Institute of Physics, Academia Sinica, Taipei 11529, Taiwan, Republic of China

(Received 12 July 2011; revised manuscript received 26 December 2011; published 31 January 2012)

Superconductivity variations deduced from the x-ray diffraction and the magnetic and heat-capacity measurements in the pseudoternary $Sr(Pd_{1-x}T_x)_2Ge_2$ layer system [Pd($4d^8$), T = Co($3d^7$), Ni($3d^8$), or Rh($4d^7$); $0 \leqslant x \leqslant 1$] are reported. For the $BaFe_2As_2$-type tetragonal structure, the degenerate nd^7 or nd^8 orbitals of transition metal T are split by c-axis squeezed TGe_4 tetrahedral crystal field in the T-Ge layer. For the isoelectronic $Sr(Pd_{1-x}Ni_x)_2Ge_2$ system, the superconducting transition temperature T_c decreases monotonically from 3.12 K for $4d$-band $SrPd_2Ge_2$ to 0.92 K for $3d$-band $SrNi_2Ge_2$, where major contributions of conduction electrons are from the half filled dispersive three-dimensional (3D)-like upper-lying $nd_{xz,yz}$ bands. For the $Sr(Pd_{1-x}Rh_x)_2Ge_2$ system, T_c decreases to 2.40 K with 25% of $4d^7$ Rh substitution. For the $Sr(Pd_{1-x}Co_x)_2Ge_2$ system, T_c decreases sharply to 2.58 K with only 3% of $3d^7$ Co substitution. No superconductivity is expected for $SrRh_2Ge_2$ and $SrCo_2Ge_2$ with lower density of states in $d_{xz,yz}$ bands due to down shift of Fermi energy E_F by one less electron per transition metal. The lower T_c of the present electron-overdoped (nd^7 or nd^8) compound is due to dispersive 3D-like $nd_{xz,yz}$ conduction bands with weak electron correlation, in comparison with the less-electron-doped ($3d^{6.1}$) 22-K superconductor $BaFe_{1.8}Co_{0.2}As_2$ or the hole-doped ($3d^{5.9}$) 38-K superconductor $Ba_{0.6}K_{0.4}Fe_2As_2$ where electron contribution is from less dispersive 2D-like lower-lying $3d_{xy}$ conduction band with stronger electron correlation.

DOI: 10.1103/PhysRevB.85.024538 PACS number(s): 74.70.−b, 61.05.cp, 61.66.Fn, 74.62.Dh

I. INTRODUCTION

The recent discovery of high superconducting transition temperatures T_c up to 55 K in the electron-correlated layer system $LaFeAs(O_{1-x}F_x)$ had generated profound interest in the superconducting FeAs-based systems.[1]

For the AFe_2As_2 (122) (A = Ca, Sr, or Ba) layer system with the $ThCr_2Si_2$-type body-centered-tetragonal (bct) structure and space group $I4/mmm$, $(FeAs)^{1-}$ layers are separated by A^{2+} layers. The parent compound $BaFe_2As_2$ is a poor metal with an antiferromagnetic spin-density wave (SDW) transition at $T_N = 140$ K. T_c up to 38 K were reported in the hole-doped $(Ba_{0.6}K_{0.4})Fe_2As_2$ and $(Sr_{0.6}K_{0.4})Fe_2As_2$, in which one $4s$ valence electron in K^{1+} substituted two $6s$ valence electrons in A^{2+},[2,3] and T_c up to 22 K were reported by the electron-doped $BaFe_{1.8}Co_{0.2}As_2$, in which seven $3d$ valence electrons in Co substituted six $3d$ valence electrons in Fe.[4–6]

For $BaFe_{1.8}Co_{0.2}As_2$ superconductor with anomalous tetragonal $c/a = 3.275$ due to squeezed $FeAs_4$ tetrahedron along the c axis, major carriers are electrons from Hall effect measurement. The local-density approximation (LDA) band calculation indicates that $3d$ electron density of states (DOS) has a downward shift on Co-$3d^7$ bands with stronger Co-$3d^7$-As-$4p$ hybridization. The LDA Fermi surface shows low dispersive two-dimensional (2D)-like d bands and Co affects the states forming heavy-hole-like bands at zone center, not on lighter electronlike bands around the zone boundary.[4–6]

The $A(Fe_{1-x}Co_x)_2As_2$ pseudoternary phase diagram (A = Ca, Sr, Ba; $0 \leqslant x < 0.13$) is similar to other high-T_c systems with a tetragonal to orthorhombic structural transition T_s before antiferromagnetic SDW transition T_N. The electron correlation strength varies from strongly correlated regime to weakly correlated regime with increasing electron doping parameter x.[7–12]

Superconductivity was also discovered in the arsenic-free ternary germanide system ST_2Ge_2 (T = transition metals) with the same $BaFe_2As_2$-type bct structure where $(PdGe)^{1-}$ layers are separated by Sr^{2+} layers.[13–19] T_c up to 3.04 K was reported for $SrPd_2Ge_2$.[15] Single-crystal $SrPd_2Ge_2$ synthesized by the metal flux method shows a lower T_c of 2.7 K with a moderate magnetic anisotropy.[19] The LDA band-structure calculation for ST_2Ge_2 (T = Pd and Ni) suggested higher dispersion energy bands across Fermi energy E_F with multi-sheet Fermi surface, and low total DOS at E_F with partial DOS contributions from T-$3d$ and Ge-$4p$.[17] Superconductivity of $SrNi_2Ge_2$ with $T_c = 0.92$ K was reported recently by our group using low-temperature resistivity measurement.[18]

In this paper, we try to answer two critical questions: (1) What is the variation of superconductivity with crystal and electronic structure in the electron-correlated layer system

$Sr(Pd_{1-x}T_x)_2Ge_2$ (T = Co, Ni, Rh)? (2) What is the origin of higher-T_c in the isostructural $Ba(Fe_{1-x}Co_x)_2As_2$ layer system?

II. EXPERIMENT

The ternary and pseudoternary $Sr(T_{1-x}T'_x)_2Ge_2$ samples (T, T' = Co, Ni, Rh, or Pd; $0 \leqslant x \leqslant 1$) were prepared by two-step arc melting under argon atmosphere. High-purity transition metals Co, Ni, Rh, and Pd (>99.9%) were arc melted with Ge (99.9999%) to form intermediate compound $(T_{1-x}T'_x)Ge$, and then melted carefully with Sr metal (99.5%). Due to high vapor pressure of Sr at the melting temperature, extra Sr was added to compensate for the evaporation loss and to ensure the stoichiometric ratio of $Sr:(T_{1-x}T'_x):Ge = 1:2:2$ to within 1%.

The x-ray powder-diffraction (XPD) data were collected by a Rigaku Rotaflex 18-kW rotating anode diffractometer with graphite monochromatized Cu-K_α radiation with a scanning step of 0.02° in the 2θ range 5°–100°.

The electrical resistivity was measured by a standard four-probe method in a ^{3}He refrigerator from 0.4 to 300 K. The magnetic susceptibility and magnetization data were collected with a Quantum Design 1-T μ-metal shielded $MPMS_2$ superconducting quantum interference device (SQUID) magnetometer from 2 to 300 K. The low-temperature heat-capacity data down to 0.3 K were collected in zero applied field and $B_a = 7$ T using the relaxation method.

For magnetic anisotropic measurements, the microcrystalline powder with average grain size $d \sim$ 1–10 μm was mixed with epoxy and aligned within a rotating quartz tube (ϕ = 8 mm) in a 0.9-T magnetic field perpendicular to the rotating axis at 300 K. The weight ratio of powder to epoxy is 1:5 and the curing time is at least 4 h. Since the tetragonal basal plane is aligned along B_a, the c axis can be in any direction perpendicular to B_a. A 10-rpm spin of the quartz tube with rotating axis normal to B_a forces the c axis of microcrystalline powders to align along the rotating axis.[20]

III. RESULTS AND DISCUSSION

The ternary SrT_2Ge_2 compounds (T = Co, Ni, Rh, Pd) crystallized with the $BaFe_2As_2$-type body-centered-tetragonal (bct) structure are shown in Fig. 1, with Sr at $(2a)$:(0, 0, 0), T at $(4d)$:(0, $\frac{1}{2}$, $\frac{1}{4}$), Ge at $(4e)$:(0, 0, z) of space group $I4/mmm$ ($Z = 2$). The $(TGe)^{1-}$ layers are separated by Sr^{2+} layers in this layer system. Within the layer, the TGe_4 tetrahedron was squeezed along the c axis, with different internal coordinates z of Ge for each metal T summarized in Table I.[13–17]

The x-ray powder-diffraction patterns are shown collectively in Fig. 2 with the corresponding tetragonal lattice parameters summarized in Table I.

Lattice parameter a and the T-T bond length $d(T\text{-}T) = a/\sqrt{2}$ decrease with decreasing transition-metal T sizes, from d(Pd-Pd) = 0.313 nm to d(Co-Co) = 0.288 nm, as shown in Table I. The long T-T bond length indicates weak direct electron T-T hopping within the T-Ge layer.

An anomalous c/a ratio increases from 2.286 for T = Pd($4d^8$) to 2.452 for Ni($3d^8$), to 2.558 for Rh($4d^7$), and to 2.624 for Co($3d^7$) due to the squeezed TGe_4 tetrahedron along the c axis, but is still smaller than c/a = 1.2980 nm/0.3964 nm = 3.275 for the isostructural $BaFe_{1.8}Co_{0.2}As_2$ superconductor.[4–6]

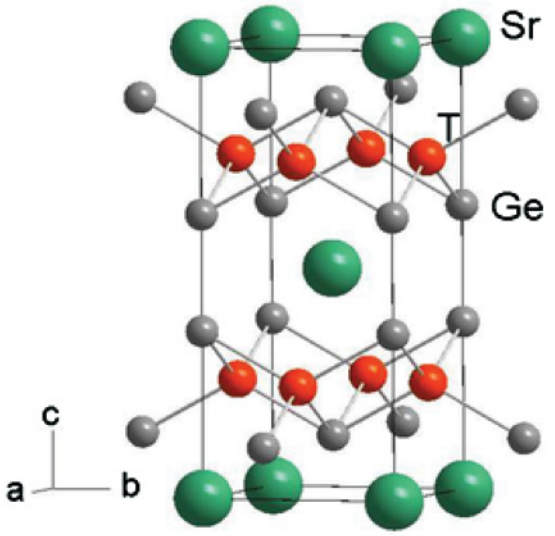

FIG. 1. (Color online) Ternary SrT_2Ge_2 compounds (T = Co, Ni, Rh, Pd) with the $BaFe_2As_2$-type body-centered-tetragonal (bct) layer structure, with squeezed TGe_4 tetrahedron along c axis.

All bond angles θ(Ge-T-Ge) in the squeezed tetrahedron along the c axis of the pseudoternary systems $Sr(Pd_{1-x}T_x)_2Ge_2$ (T = Co, Ni, Rh) are larger than 109.3° for unsqueezed ideal tetrahedron as shown in Fig. 3. A bond angle of 122.5° is observed for Pd with eight $4d$ electrons, which is similar to 122.4° for the isoelectronic Ni with eight $3d$ electrons, but is greater than 118.2° for Co with seven $3d$ electrons and 116.1° for Rh with seven $4d$ electrons.

The five degenerate nd orbitals were split into an up-lying t_{2g} triplet and a lower-lying e_g doublet in the undistorted tetrahedral crystal field with bond angle of 109.3°. In the c-axis squeezed TGe_4 tetrahedral crystal field, the t_{2g} triplet is further split into one up-lying doublet $d_{xz,yz}$ and one lower-lying d_{xy} level. The e_g doublet is split into $d_{3z^2-r^2}$ and $d_{x^2-y^2}$ levels. The conduction bands are formed by $d_{xz,yz}$ and d_{xy} orbitals with light electronlike bands from an up-lying $d_{xz,yz}$ doublet and a heavy-hole-like band from a lower-lying d_{xy} level. With eight nd electrons in T = Ni and Pd, the d_{xz} and d_{yz} bands are close to half filled, with some hole pockets in the lower d_{xy} band, and no Fermi surface is expected on lower-lying $d_{3z^2-r^2}$ and $d_{x^2-y^2}$ bands. With seven nd electrons in T = Co and Rh and a down shift of Fermi energy E_F by one less electron, the d_{xz} and d_{yz} bands are less than half filled, with some hole pockets in the lower d_{xy} band.

TABLE I. Lattice parameters summarized from the x-ray powder-diffraction data of the tetragonal SrT_2Ge_2 system (T = Pd, Ni, Rh, Co) with respective z coordinates of Ge at $(4e)$: (0,0,z).

T	z(Ge)	a (nm)	c (nm)	c/a	$d(T\text{-}T)$ (nm)
Pd	0.370	0.4420(4)	1.0104(10)	2.286	0.313
Ni	0.362	0.4181(4)	1.0251(10)	2.452	0.296
Rh	0.368	0.4193(4)	1.0724(10)	2.558	0.296
Co	0.364	0.4071(4)	1.0683(10)	2.624	0.288

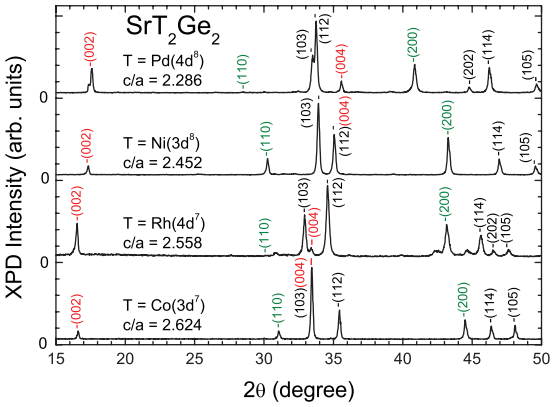

FIG. 2. (Color online) X-ray powder-diffraction (XPD) patterns for the tetragonal SrT_2Ge_2 system (T = Co, Ni, Rh, Pd), arranged in increasing c/a ratio.

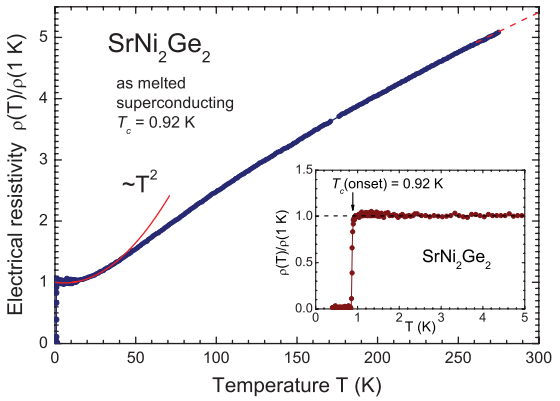

FIG. 4. (Color online) Temperature dependence of electrical resistivity ratio $\rho(T)/\rho(1\ \mathrm{K})$ of new superconductor $SrNi_2Ge_2$. Inset reveals a T_c (onset) at 0.92 K.

The T-Ge bond length $d(T\text{-Ge}) = [a^2/4 + (z - 1/4)^2c^2]^{1/2}$ as shown in the inset of Fig. 3 decreases with decreasing transition-metal T size, from 0.252 nm for Pd to 0.237 nm for Co. The short T-Ge bond length indicates strong hybridization between T-nd and Ge-4p orbitals, with delocalized, itinerant electron hopping through this channel.

The LDA band-structure calculation for SrT_2Ge_2 (T = Pd and Ni) suggests higher dispersion energy bands across Fermi energy E_F with a multisheet Fermi surface and low total DOS at E_F with partial DOS contributions from T-3d and Ge-4p. However, a small but nonzero on-site Coulomb repulsion U ($U \sim 0.5$ bandwidth W) is probably needed in the LDA + U calculations for this electron-correlated system to get a more realistic band structure. The LDA calculation expects superconductivity in $SrNi_2Ge_2$.[17] Indeed a superconducting transition temperature T_c = 0.92 K was recently observed by our group.[18] The temperature dependence of electrical resistivity ratio $\rho(T)/\rho(1\ \mathrm{K})$ for this new superconductor $SrNi_2Ge_2$ is shown in Fig. 4. With a shorter d(Ni-Ge) bond length of 0.243 nm, a lower T_c onset of 0.92 K from electrical resistivity with T_c(zero) of 0.87 K was observed with an electrical resistivity ratio $\rho(300\ \mathrm{K})/\rho(1\ \mathrm{K})$ of 5.4. The T^2 dependence of resistivity below 30 K indicates that the normal state is close to the Fermi-liquid regime with weaker electron correlation. The lower superconducting transition temperature of this electron-overdoped (nd^8) compound is probably due to more dispersive 3D-like $3d_{xz,yz}$ conduction bands, as compared with the less-electron-doped ($3d^{6.1}$) 22-K superconductor $BaFe_{1.8}Co_{0.2}As_2$ or the hole-doped ($3d^{5.9}$) 38-K superconductor $Ba_{0.6}K_{0.4}Fe_2As_2$ with less dispersive 2D-like $3d_{xy}$ conduction band.[2–6]

Figure 5 shows the low-temperature heat capacity $C(T)$ of the $SrNi_2Ge_2$ superconductor. A heat-capacity jump at T_c = 0.78 K was observed, which is slightly lower than T_c(zero) = 0.87 K measured by electrical resistivity. The C/T vs T^2 plot for zero applied field and B_a = 7 T are shown collectively in the inset. Normal-state heat capacity at B_a = 7 T can be fitted with the formula $C_N(T) = \gamma T + AT^3$, with an electronic $\gamma = 1.55 \times 10^{-2}$ J/mol K^2 and a Debye temperature θ_D = 175 K. The superconducting specific-heat jump $\Delta C/\gamma T_c$ of 1.2 is very close to the BCS value of 1.43, which suggests a fully opened s-wave-type superconducting gap for this low-T_c superconductor.

Anisotropic superconducting properties are expected for this layer system. Polycrystalline $SrPd_2Ge_2$ powder (grain size 1–10 μm) was aligned at room temperature in an alignment magnetic field of 0.9 T utilizing anisotropic paramagnetic magnetization due to the T-Ge layer structure. An easy

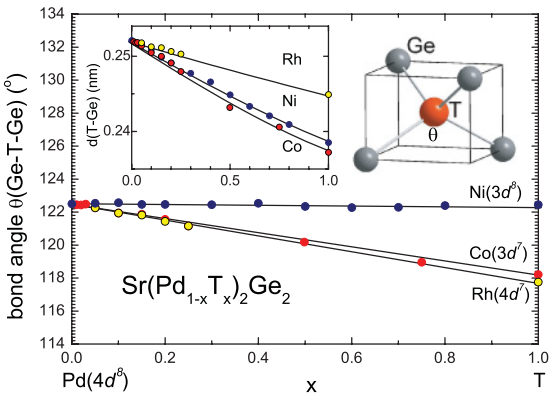

FIG. 3. (Color online) Variation of bond angle θ(Ge-T-Ge) for squeezed TGe_4 tetrahedron and bond length $d(T\text{-Ge})$ (inset) for pseudoternary systems $Sr(Pd_{1-x}T_x)_2Ge_2$ (T = Co, Ni, Rh).

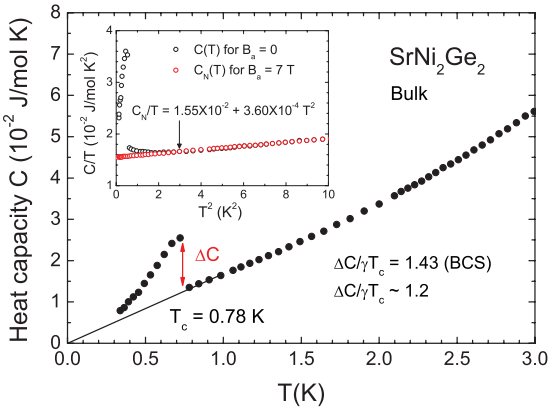

FIG. 5. (Color online) Temperature dependence of molar heat capacity $C(T)$ for superconductor $SrNi_2Ge_2$. C/T versus T^2 plot for B_a = 0 and B_a = 7 T are shown in the inset.

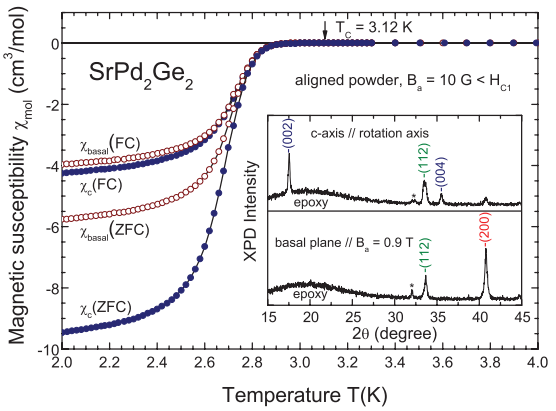

FIG. 6. (Color online) Field-cooled (FC) and zero-field-cooled (ZFC) anisotropic magnetic susceptibility $\chi_{\rm mol}(T)$ for aligned superconducting powder $SrPd_2Ge_2$ (T_c = 3.12 K). Inset shows the x-ray-diffraction patterns of aligned power along tetragonal c axis and basal plane.

magnetization direction along the tetragonal basal plane through spin-orbital coupling related magnetocrystalline anisotropy was observed.[20] The x-ray powder-diffraction (XPD) pattern for aligned powder in epoxy along the basal plane with enhanced (hk0) lines and along the c axis with enhanced (00l) lines are shown collectively in the inset of Fig. 6. Alignment was not complete probably due to intermediate alignment field strength of 0.9 T, insufficient curing time of 10 h, or simply intrinsic origin. Close to 85% alignment was achieved.

Anisotropic low-field field-cooled (FC) and zero-field-cooled (ZFC) magnetic susceptibility $\chi_{\rm mol}(T)$ for aligned powder $SrPd_2Ge_2$ (grain size 1–10 μm) along the tetragonal c axis and basal plane are shown collectively in Fig. 6. With Pd-Ge bond length d(Pd-Ge) of 0.252 nm for this electron-overdoped compound, superconducting transition T_c onset of 3.12 K was observed, which is slightly higher than the previously reported 3.04 K for bulk sample[15] and 2.7 K for single crystal.[19] At 2 K in applied field of 10 G smaller than lower critical field B_{c1}(2 K) $\sim$ 100 G,[15] a ZFC anisotropic molar susceptibility ratio χ_c(ZFC)/$\chi_{\rm basal}$(ZFC) = 9.5 cm^3 mol^{-1}/5.8 cm^3 mol^{-1} $\sim$ 1.6 at Meissner state was observed. A lower diamagnetic signal above 2.6 K is due to the small grain size where a 10-G field is already penetrated deeply into the grain.

The anisotropic initial diamagnetic magnetization curve and magnetic hysteresis loop $M(B_a)$ at $T = 2$ K $< T_c =$ 3.12 K for aligned superconducting powder $SrPd_2Ge_2$ are shown collectively in Fig. 7. The peak field penetration into microcrystalline grain center (grain size 1–10 μm) $B_{\rm basal}$(peak) is 56 G along the tetragonal basal plane and B_c(peak) is 44 G along the c axis. These peak values are slightly smaller than the average bulk B_{c1}(2 K) $\sim$ 100 G due to the lack of grain-boundary pinning for small grain size and dispersed distribution of aligned microcrystalline in epoxy. The initial magnetization curve decrease to zero around 1 kG is slightly higher than the upper critical field B_{c2}(2 K) $\sim$ 0.9 kG for the bulk sample.[15] The small hysteresis loop shown in the inset of Fig. 7 reflects the low flux pinning behavior of the dispersive microcrystalline aligned powder.

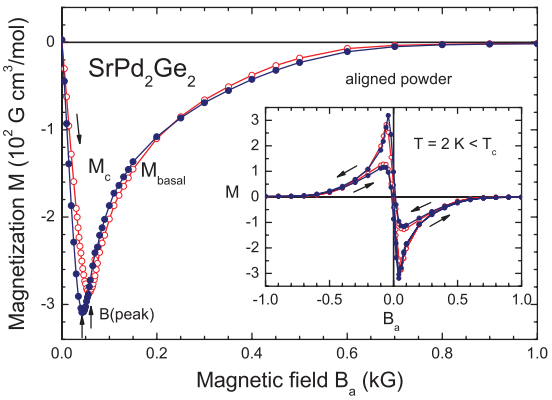

FIG. 7. (Color online) Anisotropic initial magnetization curve $M(B_a)$ and magnetic hysteresis loop (inset) at $T = 2$ K for aligned powder $SrPd_2Ge_2$ along both orientations.

Since no T_c down to 2 K were observed for less electron-doped $SrCo_2Ge_2$ and $SrRh_2Ge_2$, a systematic study of T_c variations near the Pd-rich region of the pseudoternary $Sr(Pd_{1-x}T_x)_2Ge_2$ systems (T = Co, Ni, and Rh) were performed. Figure 8 shows the T_c onset for $SrPd_2Ge_2$ and three representative compounds in the Pd-rich region. For 10% Ni substitution, T_c decreases only slightly to 3.08 K. For 10% Rh substitution, T_c decreases to 2.92 K. No T_c down to 2 K can be detected with 10% Co substitution. Lower T_c of 2.58 K was observed with only 3% Co substitution. A T_c decrease is clearly related to the decreasing electron doping in $d_{xz,yz}$ conduction bands.

Figure 9 shows variations of superconducting transition temperature T_c for all three systems. For the isoelectronic, electron-overdoped $Sr(Pd_{1-x}Ni_x)_2Ge_2$ system, T_c decreases from 3.12 K for $SrPd_2Ge_2$ with Pd($4d^8$) to 0.92 K for $SrNi_2Ge_2$ with Ni($3d^8$). For the less electron-doped $Sr(Pd_{1-x}Rh_x)_2Ge_2$ system with Rh($4d^7$), T_c decreases to 2.4 K with 25% Rh substitution and extrapolated to 65% Rh substitution at 0 K. The T_c suppression in $Sr(Pd_{1-x}Co_x)_2Ge_2$ with Co($3d^7$) was even more pronounced as T_c decreases to 2.80 K for 1% and 2.58 K for 3% Co substitution and extrapolated to 15% Co substitution at 0 K. Stronger T_c suppression for Co($3d^7$) and Rh($4d^7$) were attributed to lower DOS in conducting d

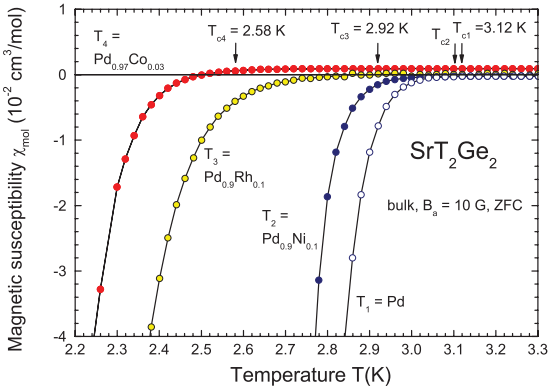

FIG. 8. (Color online) Superconducting transition temperature T_c ($\pm$0.02 K) for four representative Pd-rich $Sr(Pd_{1-x}T_x)_2Ge_2$ compounds (T_1 = Pd, T_2 = $Pd_{0.9}Ni_{0.1}$, T_3 = $Pd_{0.9}Rh_{0.1}$, and T_4 = $Pd_{0.97}Co_{0.03}$).

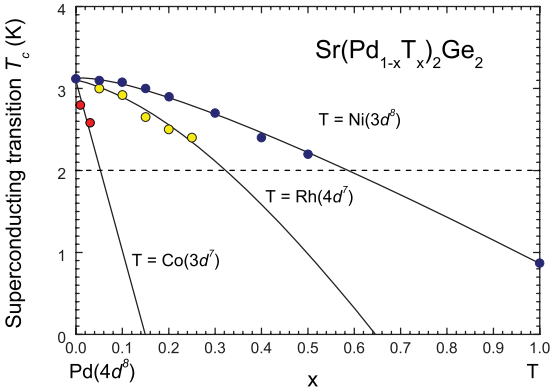

FIG. 9. (Color online) Variations of superconducting transition temperature T_c for the pseudoternary $Sr(Pd_{1-x}T_x)_2Ge_2$ system (T = Co, Ni, Rh).

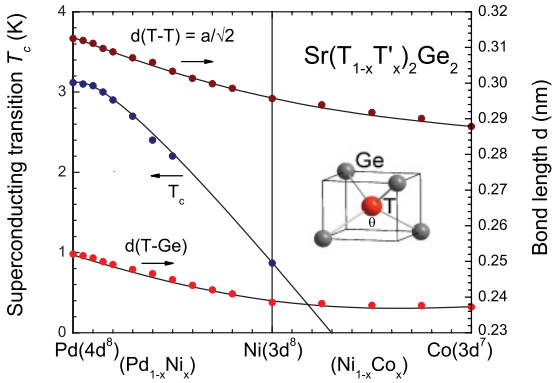

FIG. 10. (Color online) Variation of T_c and bond lengths d(T-Ge), d(T-T) of the squeezed TGe_4 tetrahedron in the $(TGe)^{1-}$ layer for $Sr(Pd_{1-x}Ni_x)_2Ge_2$ and $Sr(Ni_{1-x}Co_x)_2Ge_2$ systems.

bands while weaker T_c suppression for Ni($3d^8$) was attributed to the isoelectronic shift from the $4d$ to $3d$ band. The minor suppression in the latter system can be explained by similar band dispersion and Fermi surfaces between $SrPd_2Ge_2$ and $SrNi_2Ge_2$ compounds as indicated by band-structure calculations.[17] No superconductivity is expected for $SrRh_2Ge_2$ and $SrCo_2Ge_2$ with lower DOS in d bands due to the down shift of Fermi energy E_F (~1 eV) by one less electron per transition metal.

Figure 10 presents a variation of T_c and bond lengths $d(T\text{-Ge})$ and $d(T\text{-}T)$ of the squeezed TGe_4 tetrahedron in the $(TGe)^{1-}$ layer for pseudoternary $Sr(Pd_{1-x}Ni_x)_2Ge_2$ and $Sr(Ni_{1-x}Co_x)_2Ge_2$ systems. The $d(T\text{-}T)$ bond length decreases from 0.31(Pd) to 0.29(Ni) nm, and enhanced direct hopping in the basal plane thus suppresses the T_c.

Compared with a smaller bond angle θ(As-$Fe_{1.8}Co_{0.2}$-As) of 111.2° for 22-K superconductor $BaFe_{1.8}Co_{0.2}As_2$ with an average number 6.1 of $3d$ electrons, the greater θ values of the present system indicates that a more 2D-like d_{xy} band may contribute a higher T_c for this compound.

The symmetry of superconductivity is probably a multiband s-wave symmetry and the mechanism of superconductivity for this low-T_c system may require structural related anisotropic electron correlation with phonon mediation.

IV. CONCLUSION

The ternary and pseudoternary $Sr(T_{1-x}T'_x)_2Ge_2$ system (T, T' = Co, Ni, Rh, or Pd) is an anisotropic tetragonal layer system where nd orbitals of transition metal T are split by the squeezed TGe_4 tetrahedral crystal field. At the normal-metal state, the system is weakly electron correlated and close to the Fermi-liquid regime. The lower T_c of the anisotropic electron-overdoped 3.12-K $SrPd_2Ge_2$ and 0.92-K $SrNi_2Ge_2$ compounds are the results of close to half filled dispersive 3D-like $nd_{xz,yz}$ conduction bands. No superconductivity is expected for $SrRh_2Ge_2$ and $SrCo_2Ge_2$ compounds with a lower density of states in these bands due to one less electron per transition metal.

ACKNOWLEDGMENTS

This work was supported by Grants No. NSC98-2112-M-007-013-MY3, No. NSC99-2811-M-007-095, and No. NSC99-2112-M-003-007 of the National Science Council of the Republic of China.

*hcku@phys.nthu.edu.tw

[1] Y. Kamihara, T. Watanabe, M. Hirano, and H. Hosono, J. Am. Chem. Soc. **130**, 3296 (2008).
[2] M. Rotter, M. Tegel, and D. Johrendt, Phys. Rev. Lett. **101**, 107006 (2008).
[3] K. Sasmal, B. Lv, B. Lorenz, A. M. Guloy, F. Chen, Y.-Y. Xue, and C.-W. Chu, Phys. Rev. Lett. **101**, 107007 (2008).
[4] A. S. Sefat, R. Jin, M. A. McGuire, B. C. Sales, D. J. Singh, and D. Mandrus, Phys. Rev. Lett. **101**, 117004 (2008).
[5] D. J. Singh, Phys. Rev. B **78**, 094511 (2008).
[6] E. Aktürk and S. Ciraci, Phys. Rev. B **79**, 184523 (2009).
[7] T.-M. Chuang, M. P. Allan, J. Lee, Y. Xie, N. Ni, S. L. Bud'ko, G. S. Boebinger, P. C. Canfield, and J. C. Davis, Science **327**, 181 (2010).
[8] N. Ni *et al.*, Phys. Rev. B **78**, 014523 (2008).
[9] H. Hosono, Physica C **469**, 314 (2009).
[10] A. I. Goldman *et al.*, Phys. Rev. B **78**, 100506 (2008).
[11] S.-H. Baek *et al.*, Phys. Rev. B **79**, 052504 (2009).
[12] J.-H. Chu, J. G. Analytis, C. Kucharczyk, and I. R. Fisher, Phys. Rev. B **79**, 014506 (2009).
[13] G. Just and P. Paufler, J. Alloys Compd. **232**, 1 (1996).
[14] W. Dörrscheidt, N. Niess, and H. Schafer, Z. Naturforsch. B **31**, 890 (1976).
[15] H. Fujii and A. Sato, Phys. Rev. B **79**, 224522 (2009).
[16] H. Fujii and A. Sato, J. Alloys Compd. **487**, 198 (2009).
[17] I. R. Shein and A. L. Ivanovskii, Physica B **405**, 3213 (2010).
[18] C. D. Yang, H. C. Hsu, W. Y. Tseng, H. C. Chen, H. C. Ku, M. N. Ou, Y. Y. Chen, and Y. Y. Hsu, J. Phys.: Conf. Ser. **273**, 012089 (2011).
[19] N. H. Sung, J.-S. Rhyee, and B. K. Cho, Phys. Rev. B **83**, 094511 (2011).
[20] B. C. Chang, C. H. Hsu, Y. Y. Hsu, Z. Wei, K. Q. Ruan, X. G. Li, and H. C. Ku, Europhys. Lett. **84**, 67014 (2008).